17th World Conference on Earthquake Engineering, 17WCEE
Sendai, Japan - September 13th to 18th 2020

On the Performance of Vertical Base Isolation Systems Using an Adjustable Constant-Force Generator

M. Saitoh[(1)], Y. Sawano[(2)]

[(1)] *Professor, International Institute for Resilient Society, Saitama University, Japan, saity@mail.saitama-u.ac.jp*
[(2)] *Undergraduate student (former affiliation), Department of Civil and Environmental Engineering, Saitama University, Japan*
…

Abstract

This paper presents an innovative vertical base isolation system incorporating a newly developed constant-force generator that can vary the generated force with a simple operation. For many decades, earthquake engineers have struggled against handling the self-weight of objects when controlling them through isolators. It is apparent that even a small difference between the weight of the isolated objects and the constant force generated by a conventional constant-force generator will cause the objects to move up or down in an accelerating manner. To overcome this issue, this study proposes an adjustable constant-force generator. The generator consists of negative and positive spring systems comprising elastically stretchable shafts and sliders connecting with elastic springs. By appropriately adjusting the lengths of the shafts, spring constants, and initial strains applied to the springs, it is possible to generate target constant forces. The generator has an optional function to generate linearly varying forces that are added to the constant force, which can achieve a satisfactorily long natural period of the isolation systems. Various spring constants of the linearly varying forces can be accomplished by changing the strain of the spring in the shaft comprising the positive spring system. The analytical solution shows that an approximate but almost exact constant force can be achieved by coupling the forces of the two systems. In addition, a demonstrator of the proposed force generator is constructed to confirm the proposed solution. This paper finally presents the performance of the vertical isolation system by conducting vertical shaking table experiments using the demonstrator. The results of the experiments show that the proposed system properly supports the isolated objects, and the response acceleration of the isolated object appreciably decreases when subjected to various observed earthquake ground motions of the up-down component. This implies that a combination of the proposed vertical isolation system and ordinary two-dimensional horizontal isolation systems may achieve a real three-dimensional base isolation system.

Keywords: Vertical base isolation, vertical ground motions, constant-force generators, 3-dimensional base isolation systems

1. Introduction

For many decades, earthquake engineers have struggled against handling the self-weight of objects when realizing vertical base isolation systems to prevent from vertical excitations. It is apparent that even a small difference between the weight of the objects and the constant force generated by a conventional constant-force generator will cause the objects to move up or down in an accelerating manner. In general, extra energy is necessary to keep the objects still or to move them against gravitational acceleration. Since the development of the Anglepoise lamp, a well-known counter-balancing system, by the engineer George Carwardine in the early 1930s, various types of counter-balancing systems or constant-force generators have been proposed for the purpose of eliminating the effect of the self-weight of objects. The history and the mechanism of the spring-and-lever balancing type systems represented by the Anglepoise lamp were well summarized by French and Weddin [1]. These systems utilizing normal springs result in approximate balance or require more complex adjustment mechanisms. To improve this approximation, te Riele and Herder [2] achieved perfect balance with normal springs directly attached to the links of simple mechanisms. Instead of using normal springs, the incorporation of so-called “zero-free-length” springs is a more common

recent trend for accomplishing perfect static balance (e.g., Hain [3], Nathan [4], Tuijthof and Herder [5]). Another method, which is rather primitive, is counter-weight balancing type systems: Mahalingam and Sharan [6] studied the advantages and disadvantages of the various systems, pointing out that the total weight of the system and the unbalance moment of the lower arm in manipulators are increased by the mass balancing.

A further extension of force generators may be expected not only to support the self-weight of the objects but also to generate additional slope forces that achieve a sufficiently long natural period of the isolation systems at the same time. For the purpose, Saitoh [7] proposed a constant-force generator with slope forces using positive and negative spring systems constructed using normal compression and tension springs. This extension will give an equilibrium at the neutral position to objects having fluctuating isolated objects owing to the additional stiffness. Moreover, the proposed force generator has a function of adjusting the amount of the constant force by a very simple manner, which can easily take the balance between the weight of the object and the supporting force.

The objectives of this study are: (1) to present the analytical solution of the constant-force generator with slope forces; (2) to construct a demonstrator of the generator; and (3) to present the performance of the vertical isolation system by conducting vertical shaking table experiments using the demonstrator.

2. Mechanics of Adjustable Constant-Force Generator with Slope Forces

2.1 Configuration of Generator

The mechanical system of the constant-force generator with slope forces proposed in this study is shown in Fig. 1. The system consists of two parts: a positive spring system and a negative spring system. Each system is commonly composed of an elastically-stretchable shaft (hereinafter, “Shaft-P” for the positive system and “Shaft-N” for the negative system), and a slider connecting with an elastic spring (hereinafter, “Spring-IP” for the positive system and “Spring-IN” for the negative system). The stretchable shaft can simply be constructed using a rigid rod, a corresponding fitting rod, and an elastic normal spring. For instance, the rigid rod is placed inside the fitting rod, which has a hollow shape with a closed tip and has a larger inner diameter than the outer diameter of the rigid rod. The spring is placed between the rods, and the two ends of the spring are connected to the rods. A compression or tension shaft can be constructed by changing the type of spring inserted in the shaft (hereinafter, “Spring-SP” for the positive system and “Spring-SN” for the negative system). The tip of the shaft is hinged at a vertical column whose tip is perfectly fixed at the base. The other end of the shaft is hinged to the slider. The slider is placed on a plate, and the slider can slide in one direction on the plate through a slide guide. The plate is a loading plate in the system, which is free to move in the vertical direction and is fixed in the other directions. These boundary conditions of the plate can be achieved by applying an appropriate slide guide in the vertical direction, as shown in Fig. 1. The main concept of the method for generating a constant force using these positive and negative spring systems is explained below.

In the system, the force generated from the shaft is transmitted to the slider, and its horizontal component is in equilibrium with a force generated from Spring-IP or -IN with an appropriate strain. One the one hand, an unbalanced force remains in the vertical direction and is transmitted to the loading plate. The unbalanced forces generated in both positive and negative systems are somehow cancelled out and flattened or sloped with an appropriate combination of the spring constants and their initial strains in the systems. To accomplish a constant force, the stiffness generated from the positive spring system needs to be the same value as, but the opposite sign to, the negative one.

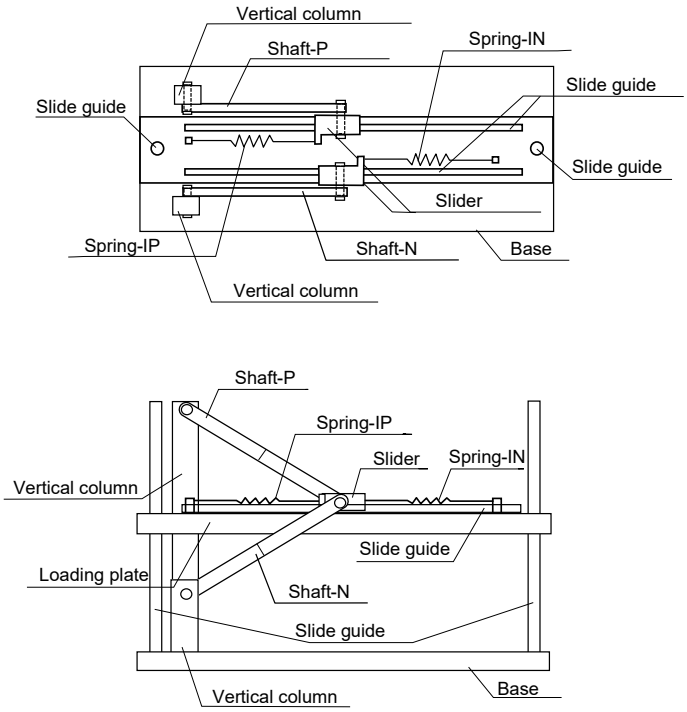

Fig. 1 Schematic diagram of proposed force generator.

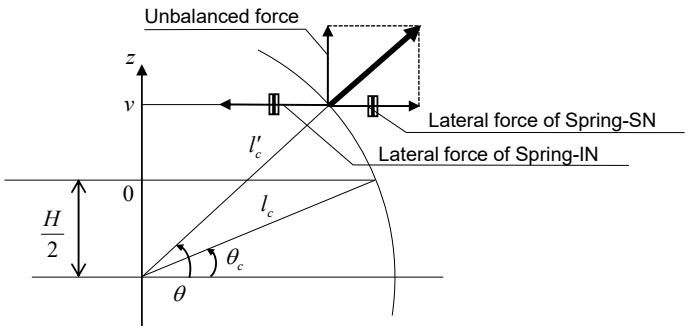

Fig. 2 Diagram showing mechanism of negative spring system.

2.2 Negative Spring System

A diagram of the negative spring system is shown in Fig. 2. The origin of the z -axis is located at the center of the hinged ends of Shaft-P and Shaft-N, where the distance between the two ends is denoted as H. Therefore, the center of rotation of Shaft-N is located at $z = -H/2$. The angle of the shaft with respect to the horizontal line is denoted as θ. In this study, the initial conditions are defined when the end of the shaft connecting with the slider is located at $z = 0$ ($\theta = \theta_c$). The length of the shaft is denoted by l_c, the spring constant and initial strain of Spring-SN at the initial position are denoted k_s and Δl_0, and those of Spring-

IN are denoted by K_I and Δl_I. To generate the unbalanced force in the positive z direction in this system, a compressive strain is given to Spring-SN. Herein, compressive strain of the springs used in the negative spring system is defined as positive. The unbalanced force in the vertical direction and the displacement of the loading plate from the initial position are denoted as F_v and v, respectively.

In Saitoh [7], it was derived that the following force-displacement relationship can be obtained when the spring constant K_I and the initial strain of Spring-IN Δl_I satisfy Eq. 3 and Eq. 4, respectively.

$$F_v(v) = K_v\left(\frac{H}{2} + v\right) \tag{1}$$

where

$$K_v = k_s \frac{\Delta l_0}{l_c} \tag{2}$$

$$K_I = k_s \frac{\Delta l_0}{l_c} \tag{3}$$

$$\Delta l_I = l_c \cos\theta_c \tag{4}$$

Eq. 1 shows that this unbalanced force is proportional to the position v, and the positive force is generated with positive v and vice versa. This behavior is completely opposite to that of a normal positive spring: in other words, this system perfectly behaves as a negative spring system.

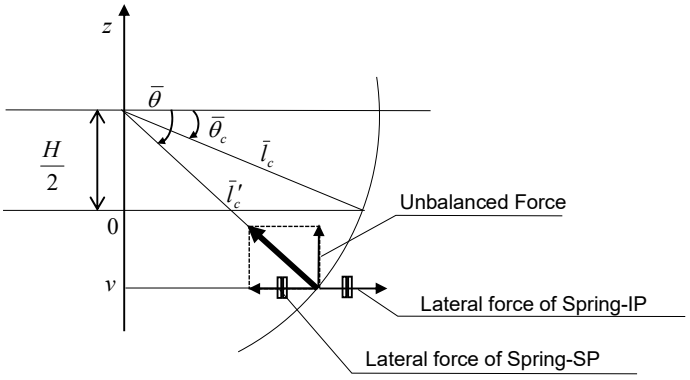

Fig. 3 Diagram showing mechanism of positive spring system.

2.3 Positive Spring System

Fig. 3 shows a diagram of the positive spring system. Basically, the mechanical configuration of this system is symmetric about the center line $v = 0$. The center of rotation of Shaft-P is located at $z = H/2$. The angle of the shaft with respect to the horizontal line is denoted as $\bar{\theta}$, where the clockwise direction is defined as positive. To generate the unbalanced force in the positive z direction in this system, a tension strain is given to Spring-SP. The tension strain of the springs used in the positive spring system is defined as

positive. Note that all the variables corresponding to those in the negative spring system are denoted using the same symbols with an over bar.

In Saitoh [7], along the same lines as the derivation of the negative spring system, the following force-displacement relationship was obtained when the spring constant $\overline{K}_I$ and the initial strain of Spring-IN $\Delta\overline{l}_I$ satisfy Eq. 7 and Eq. 8, respectively.

$$\overline{F}_v(v) = \overline{K}_v\left(\frac{H}{2} - v\right) \tag{5}$$

where

$$\overline{K}_v = \bar{k}_s \frac{\Delta\bar{l}_0 + \Delta\bar{l}_c}{\bar{l}_c + \Delta\bar{l}_c} \tag{6}$$

$$\overline{K}_I = \bar{k}_s \frac{\Delta\bar{l}_0}{\bar{l}_c} \tag{7}$$

$$\Delta\bar{l}_I = \bar{l}_c \cos\bar{\theta}_c \tag{8}$$

In Eq. 6, the increment in the shaft length, $\Delta\bar{l}_c$, more or less affects the consistency of the stiffness $\overline{K}_v$: the discrepancy between Eq. 2 and Eq. 6 is attributed by a mechanical asymmetricity of the two systems. The effect of $\Delta\bar{l}_c$ is negligibly small when the length of the shaft $\bar{l}_c$ and the initial tension strain $\Delta\bar{l}_0$ are taken as large values. In this case, the stiffness $\overline{K}_v$ can be approximated as follows:

$$\overline{K}_v \cong \bar{k}_s \frac{\Delta\bar{l}_0}{\bar{l}_c} \tag{9}$$

2.4 Adjustable Constant-Force Generator

The negative spring system and the positive spring system derived in the previous subsections are combined to construct a constant-force generator. The total force of both unbalanced forces from the systems are expressed in terms of Eq. 1 and Eq. 5 as

$$f_v(v) = F_v(v) + \overline{F}_v(v) = K_v\left(\frac{H}{2} + v\right) + \overline{K}_v\left(\frac{H}{2} - v\right) \tag{10}$$

Eq. 10 can be rewritten in the following form:

$$f_v(v) = \frac{1}{2}\left(K_v H + \overline{K}_v H\right) + \left(K_v - \overline{K}_v\right)v \tag{11}$$

It is apparent that the first term on the right side in Eq. 11 represents a constant force f_0 at $v = 0$, whereas the second term represents a slope force in terms of position v. The corresponding slope of the force k_m is expressed as

$$k_m = K_v - \overline{K}_v \tag{12}$$

Therefore, the total force f_v is in general a truncated shape where the slope force can vary with k_m ranging from positive to negative according to Eq. 12.

To realize a constant force in the system, applying the conditions $l_c = \bar{l}_c, k_s = \bar{k}_s$ and $\Delta l_0 = \left|\Delta \bar{l}_0\right|$ to Eq. 11 yields

$$f_v \cong k_s \frac{\Delta l_0}{l_c} H = const. \tag{13}$$

Eq. 13 indicates that the total force is approximately constant when the increment in the length of the shaft, $\Delta \bar{l}_c$, is negligibly small. Note that, satisfying these conditions is not technically difficult in practice. For the variability of the constant force, Eq. 13 implies that the amplitude of the constant force depends on four components: k_s, l_c, Δl_0 and H. Of these variables, one that is easy to vary in practice is the distance H, as there are many types of adjusters in industrial products for changing the distance between two hinges, such as a screw-shaft etc. In this case, the constant force is in direct proportion to the distance H, which can take even negative quantities. Therefore, a very wide range of adjustability of the constant force can be accomplished in this system.

2.5 Verification of Adjustable Constant-Force Generator

Fig. 4 shows the variations of the constant force by adjusting the distance H. The target constant force is initially set to $f_v = 6.00$ N. By using Eq. 11, the corresponding variables are determined as follows: $l_c = \bar{l}_c = 300$ mm, $k_s = \bar{k}_s = 0.102$ N/mm, $\Delta l_0 = \Delta \bar{l}_0 = 117.7$ mm and $H = \overline{H} = 150$ mm. The range of the position v computed here is set from $-H/2$ (-75 mm) to $H/2$ (+75 mm). In this computation, other two distances are considered by setting H =100 mm (4.00 N) and 50 mm ($f_v = 2.00$ N). Fig. 4 shows that these target forces are achieved with reasonable accuracy by changing the distance.

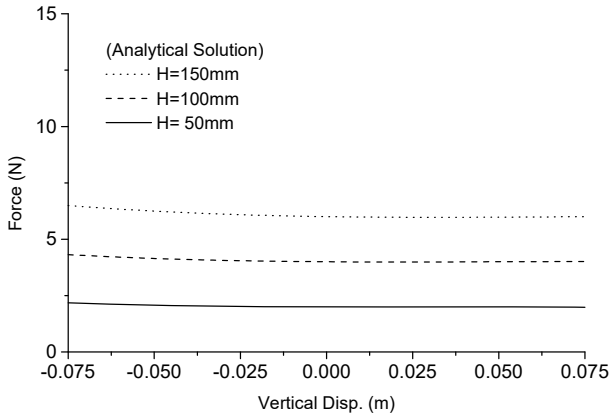

Fig. 4 Analytical solution of proposed adjustable constant-force generator by adjusting distance

3. Demonstration of Constant-Force Generator and Vertical Base Isolation Systems

3.1 Performance of Constant-Force Generator

To confirm the theory of the proposed constant-force generators, a demonstrator was manufactured, as shown in Fig. 5. This demonstrator was designed to have a similar configuration to the mechanical system shown in Fig. 1. Moreover, a function to change the distance H is incorporated to confirm the performance of variations in constant forces. A distance adjuster consists of a typical trapeziform screw shaft, two trapezoidal female screws, and a grip for rotating the shaft. The tips of Shaft-P and Shaft-N are hinged at the trapezoidal female screws, respectively. By rotating the grip, the screw shaft rotates, and the distance between the female screws can be changed. In this paper, therefore, the performance of constant-force generation and the function of constant-force adjustment by changing the height are demonstrated below.

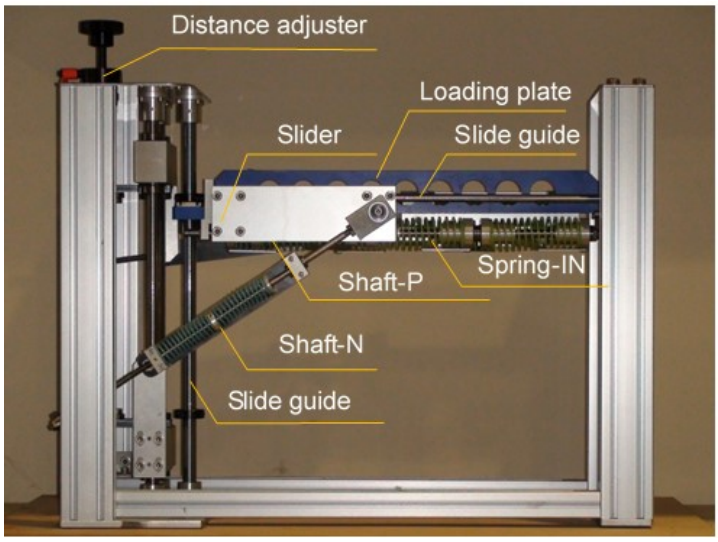

Fig. 5 Demonstrator of proposed constant-force generator.

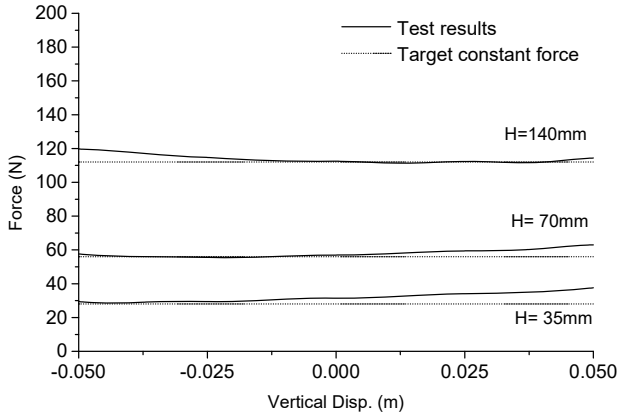

Fig. 6 Experimental results of force and displacement relations obtained from monotonic loading tests using demonstrator of constant-force generator.

Monotonic loading tests were conducted using the demonstrator. In the tests, the loading plate was connected to a digitally controlled unidirectional hydraulic actuator (±10 kN, ±150 mm) and was quasi-statically (5 mm/s) loaded from v =+50 mm to -50 mm. Measured data of reaction forces associated with the loading displacement were passed through a digital low-pass filter to remove the effects of noise from

the recorded data. Herein, the effects of the self-weight of the mechanical parts vertically moving with the head of the actuator were removed from the measured forces. In the tests, the target constant force was initially set to $f_v = 112$ N. The corresponding variables were determined from Eq. 11, and the obtained properties in the real system were as follows: $l_c = \bar{l}_c = 300$ mm, $k_s = \bar{k}_s = 2.045$ N/mm, $\Delta l_0 = \Delta \bar{l}_0 = 117.7$ mm, $K_1 = \bar{K}_1 = 0.793$ N/mm, and $H = 140$ mm.

Fig. 6 shows the generated forces and position v relations obtained from the tests. The graph indicates that, as a whole, this demonstrator appropriately generates constant forces within the loading range of displacement. At the neutral position, the generated force is 111 N, which is fairly close to the target force. By changing the distance H from 140 mm to 70 mm, the generated forces tend to reduce to about one-half of the initial forces (57.3 N at $v = 0$). This implies that the demonstrator properly follows the theory proposed in this study. The figure also shows that further reduction of the distance to 35 mm (one-quarter of the initial distance) generates approximately one-quarter of the initial force (31.5 N at $v = 0$).

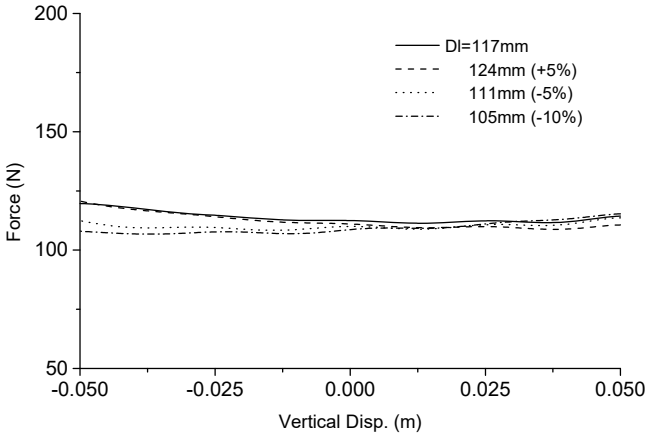

Fig. 7 Experimental results of truncated force-displacement relations obtained from monotonic loading tests using demonstrator of constant-force generator with variable stiffness by changing initial strain of Spring-SP.

Furthermore, this demonstrator was used to confirm the variability of the spring constant k_m by changing the initial strain of Spring-SP. It is known that that the spring constant k_m varies widely with a change in the strain of Spring-SP [7]. In this experiment, the initial strain of Spring-SP was controlled as strains with -5%, 5%, and 10% increments from $\Delta l_0 = 117.7$ mm. These extreme increments in positive and negative directions are compatible to the allowable limitation of this mechanical spring system. The distance H was kept as 140 mm. Note that, in this case, the constant force f_v changes in accordance with the change in the initial strain of Spring-SP: no adjustment of the distance H to maintain a consistent constant force was conducted in the tests in order to remove the effects of such adjustment from the results.

Fig. 7 shows the generated force and position v relations with different spring constants k_m ranging from positive to negative values with the initial strains of Spring-SP. The results indicate that this demonstrator appropriately generates a force having a truncated shape. In addition, although the variable stiffness is properly demonstrated, the range of variation in stiffness is somewhat narrow due to restrictions in this demonstrator.

3.2 Performance of Vertical Base Isolation System

In this subsection, this demonstrator was used to perform a base isolation function when subjected to vertical excitations. Fig. 8 shows a base isolation system consisting of the demonstrator and a steel weight of 11.9kg as an isolated object which was placed on the loading plate. In the system, $\Delta l_0 = \Delta \bar{l}_0 = 117.7$ mm and $H = 140$ mm were initially applied, then a subtle amount of adjustment of the distance was manipulated to take a balance between the weight and the force of the generator. As shown in Fig. 7, a slop stiffness was intrinsically achieved a satisfactorily long natural period: natural frequencies vary with a range from about 0.2Hz to 1.0Hz. This frequency range was confirmed by a separately conducted vibration test using a sweep wave.

In this experiment, the base of the demonstrator was fixed to a firm frame box, and the top of the box was connected to the actuator in the vertical direction as shown in Fig. 8. Two recorded ground motions of UD component were applied from the actuator in the form of displacement (e.g., displacement control). In this experiment, 2016 Kumamoto earthquake records at KIK-NET station (KMMH16: Mashiki) [8] were used. In the event of the earthquake, two large ground motions were recorded at the station during a foreshock (14/Apr./2016) and the main shock (16/Apr./2016). The two accelerometers were applied to the frame and the isolated object to measure the vertical acceleration responses. It is noted that a local resonance of the frame box appeared around 20Hz as an inherent characteristic, which disturbed rational observation of the responses. So, a 20Hz low-pass filter was applied to the acceleration records. This procedure may not distort the main signal as the frequencies above 20Hz is far beyond the dominant frequency range of the input and the base isolation system.

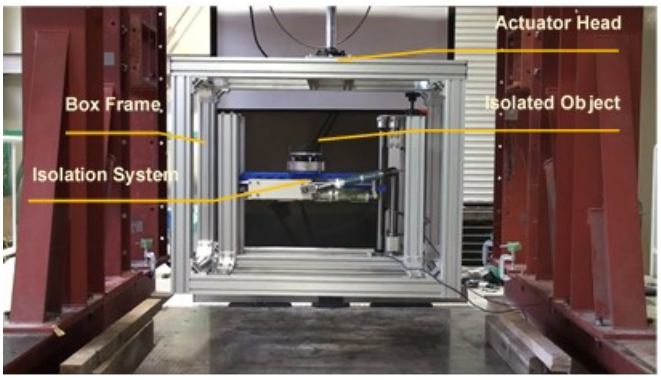

Fig. 8 Demonstrator of vertical base isolation system using proposed constant-force generator.

Fig. 9 shows the time-history acceleration responses of the frame as the UD input and the isolated object when subjected to the record on 14/Apr./2016. The figure also shows the time-history displacement response of the object with respect to the frame. This displacement was computed by integrating the time-history relative acceleration of the object with respect to the frame. The figure shows that the maximum amplitude of the input was 11.49m/s^2 while the maximum amplitude at the isolated object was 2.46m/s^2: a satisfactory decrease in the acceleration can be achieved. The maximum amplitude of the relative displacement was 0.0277m, which is far below the allowable limit of the system ($\pm$0.75mm).

In case of applying the record on 16/Apr./2016, Fig. 10 also shows an appreciable decrease in the acceleration, which is commensurate with the case of record on 14/Apr./2016. Although only two cases were presented in this application example, the results indicate that this proposed vertical base isolation system has a high potential to decrease markedly the acceleration response of isolated objects.

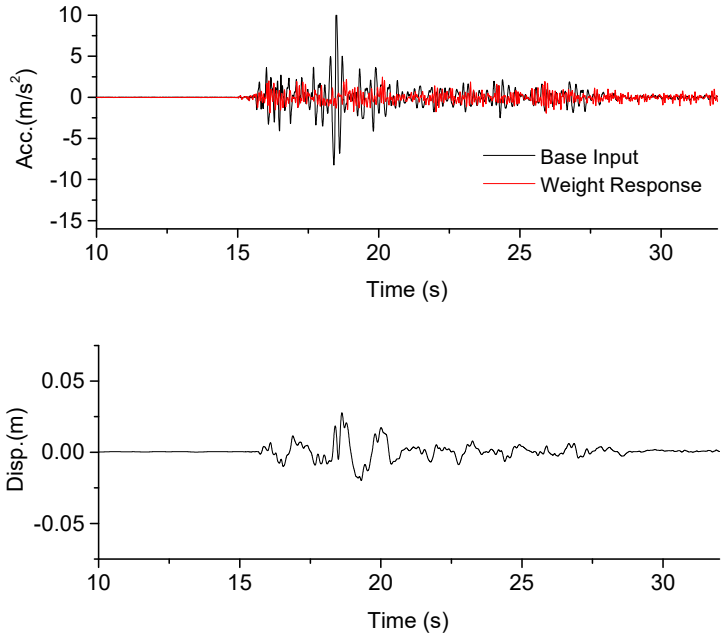

Fig. 9 Experimental results of base input and isolated weight responses when subjected to observed record of UD component at KIK-NET station (KMMH16 on 14/Apr./2016).

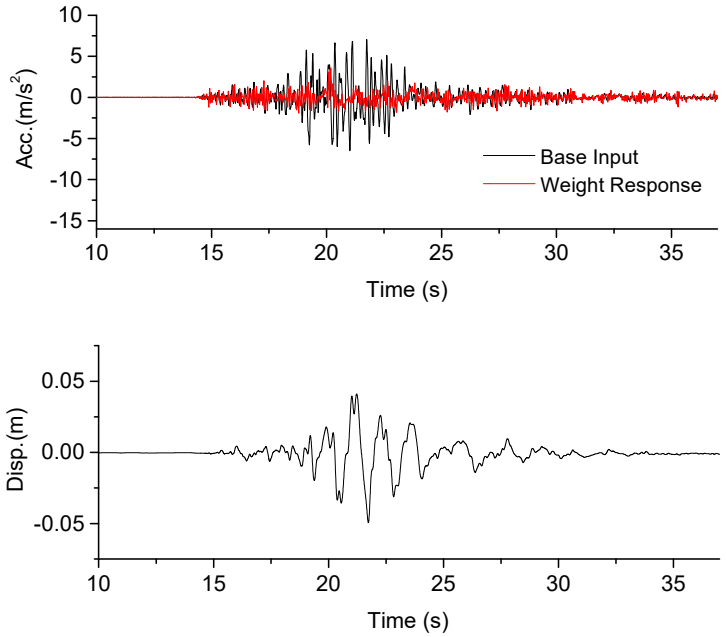

Fig. 10 Experimental results of base input and isolated weight responses when subjected to observed record of UD component at KIK-NET station (KMMH16 on 16/Apr./2016).

4. Conclusions

This study proposed an adjustable constant-force generator using positive and negative spring systems constructed using normal compression and tension springs. Each system was composed of an elastically stretchable shaft, a slider connecting with an elastic spring, and a loading plate connecting with the shaft and slider. An unbalanced force perfectly proportional to the position of the loading plate can be generated in the negative spring system. Moreover, an unbalanced force approximately proportional to the position of the loading plate can be generated in the positive spring system in the same manner. An approximate but almost exact constant force can be achieved by coupling the forces of the two systems. To accomplish an adjustable constant force by using the present system, the distance between the hinges of the elastically stretchable shafts in both systems was changed: the constant force changed in direct proportion to the change in the distance, which can take even negative distances. The proposed system was extended to generate slope forces in addition to the constant forces simultaneously. In the extended system, a change in the spring constant was accomplished by applying extra strain energy in the positive spring system by changing the initial strain of the springs.

The analytical solutions of the proposed systems showed that an approximate but almost exact constant force can be achieved by coupling the forces of the two systems. A demonstrator of the proposed force generator was constructed to confirm the proposed theory by conducting monotonic loading tests. The results indicated that constant forces were appropriately adjusted by changing the distance between the hinges of the spring shafts. Moreover, the demonstrator created a truncated shape of forces: the variable stiffness was properly demonstrated by changing the initial strain of the positive spring shaft.

Finally, the demonstrator was applied to a vertical base isolation system subjected to vertical excitations. The results of the experiments showed that the proposed system appropriately supported the isolated objects, and the response acceleration of the isolated object satisfactorily decreased when subjected to observed earthquake ground motions of the up-down component. Consequently, the test results implied that the proposed vertical base isolation system is promising.

5. Acknowledgements

The strong motion data used in this study were provided by the National Research Institute for Earth Science and Disaster Prevention (NIED, KIK-NET).

6. References

[1] French, M. J., Widden, M. B. (2000): The Spring-and-Lever Balancing Mechanism, George Carwardin and the Anglepoise Lamp, Proc. Inst. Mech. Eng., Part C: J. Mech. Eng. Sci. 214 501–508.

[2] te Riele, F. L. S, Herder, J. L. (2001): Perfect Static Balance with Normal Springs, , Proc. Of DETC'01, ASME2001, Design Engineering Technical Conferences and Computers and Information in Engineering Conference, Pittsburgh, Pennsylvania, DETC2001/DAC-21069 1–8.

[3] Hain, K (1952): Der Federausgleich von Lasten, Grundlagen der Landtechnik, (3)38/50.

[4] Nathan, R. H. (1985): A constant force generating mechanism, Journal of Mechanisms, Transmissions, and Automation in Design, 107(12)508/12.

[5] Tuijthof, G. J. M., Herder, J. L (2000): Design, actuation and control of an anthropomorphic robot arm, Mechanism and Machine Theory 35(7)945-962.

[6] Mahalingam, S., Sharan, A. M. (1986): The optimal balancing of the robotic manipulators, IEEE international conference on robotics and automation, 828-835.

[7] Saitoh, M. (2015): ELASTIC MECHANISM, Patent, Foreign Code F170009133, Priority Data P2015-175377 (Sep 7, 2015) JP.

[8] National Research Institute for Earth Science and Disaster Resilience (2019), NIED K-NET, KiK-net,National Research Institute for Earth Science and Disaster Resilience, doi:10.17598/NIED.0004

